On the Nature of the Mesoscale Variability in Denmark Strait

WILKEN-JON VON APPEN

Alfred Wegener Institute Helmholtz Centre for Polar and Marine Research, Bremerhaven, Germany

DANA MASTROPOLE AND ROBERT S. PICKART

Department of Physical Oceanography, Woods Hole Oceanographic Institution, Woods Hole, Massachusetts

HÉÐINN VALDIMARSSON

Marine Research Institute, Reykjavík, Iceland

STEINGRÍMUR JÓNSSON

University of Akureyri, Akureyri, and Marine Research Institute, Reykjavík, Iceland

JAMES B. GIRTON

Applied Physics Laboratory, University of Washington, Seattle, Washington

(Manuscript received 28 May 2016, in final form 20 December 2016)

ABSTRACT

Time series data from a mooring in the center of Denmark Strait and a collection of shipboard hydrographic sections occupied across the sill are used to elucidate the mesoscale variability of the dense overflow water in the strait. Two dominant, reoccurring features are identified that are referred to as a bolus and a pulse. A bolus is a large, weakly stratified lens of overflow water associated with cyclonic rotation and a modest increase in along-stream speed of $0.1 \, \mathrm{m \, s^{-1}}$. When a bolus passes through the strait the interface height of the overflow layer increases by 60 m, and the bottom temperature decreases by 0.4°C. By contrast, a pulse is characterized by anticyclonic rotation, a strong increase in along-stream speed of $>0.25 \, \mathrm{m \, s^{-1}}$, a decrease in interface height of 90 m, and no significant bottom temperature signal. It is estimated that, on average, boluses (pulses) pass through the strait every 3.4 (5.4) days with no seasonal signal to their frequency. Both features have the strongest along-stream signal in the overflow layer, while the strongest cross-stream velocities occur above the Denmark Strait overflow water (DSOW). In this sense neither feature can be characterized as a simple propagating eddy. Their dynamics appear to be similar to that ascribed to the mesoscale variability observed downstream in the deep western boundary current. Strong correlation of bottom temperatures between the mooring in Denmark Strait and a downstream array, together with a match in the frequency of occurrence of features at both locations, suggests a causal relationship between the mesoscale variability at the sill and that farther downstream.

1. Introduction

Denmark Strait overflow water (DSOW) is the largest and densest component of North Atlantic Deep Water (NADW) and contributes significantly to the deep limb of the global overturning circulation (Dickson and Brown 1994; Hansen and Østerhus 2007). There are two different paradigms by which this water is formed within the Nordic Seas. The first involves the boundary current system encircling the interior basins (Mauritzen 1996). Specifically, warm and salty water from the Gulf Stream/
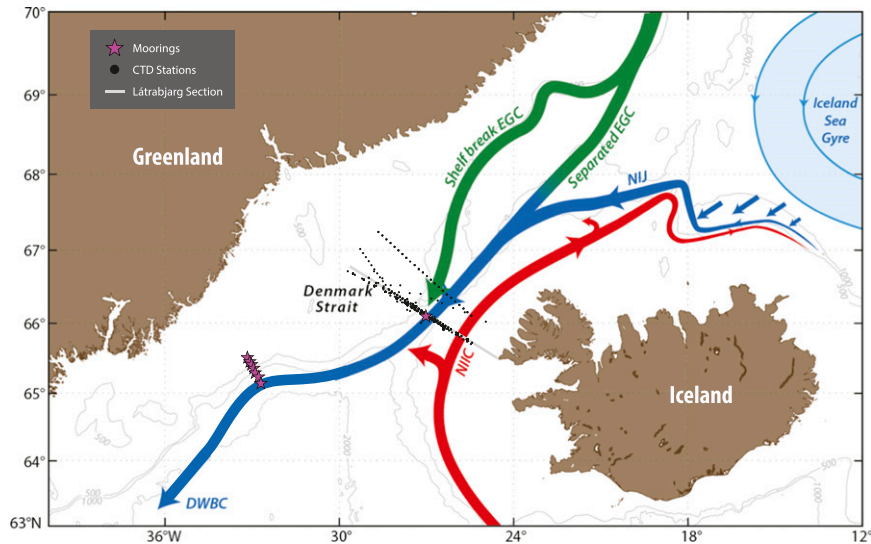
FIG. 1. Schematic of currents flowing through Denmark Strait and various place names. The magenta stars are mooring DS1 in Denmark Strait and moorings EG1–EG7 along the Spill Jet line. The Látrabjarg line, located near the sill, is drawn in gray. The black dots are the CTD stations composed of the 111 shipboard transects used in the study (the majority of which are along the Látrabjarg line). The 500-, 1000-, and 2000-m isobaths are contoured in light gray.

North Atlantic Current crosses the Greenland–Scotland Ridge and flows northward in the Norwegian Atlantic Current. Strong air–sea heat loss densifies the water, some of which recirculates in the vicinity of Fram Strait (Hattermann et al. 2016), joins the East Greenland Current (EGC), and flows southward to Denmark Strait. This is known as the rim current overturning loop, and the overflow water so produced is referred to as Atlantic-origin water. The second paradigm for dense water formation involves convection in the interior basins, which produces a water mass known as Arctic-origin water (with very different temperature–salinity characteristics than the Atlantic-origin overflow; e.g., Swift and Aagaard 1981; Våge et al. 2011). It has been argued that Arctic-origin overflow water emanates from both the central Iceland Sea (Swift and Aagaard 1981) and the central Greenland Sea (Strass et al. 1993). The model results of Våge et al. (2011) imply that there is a second Nordic Seas overturning loop, local to the Iceland Sea, that converts the warm and salty water of the north Icelandic Irminger Current (NIIC) into this class of overflow water.

The dense water formed north of the Greenland–Scotland Ridge is carried into Denmark Strait via a set of three currents: the shelfbreak EGC; the separated EGC, which bifurcates from the shelfbreak branch north of the Blosseville Basin (Våge et al. 2013); and the north Icelandic jet (NIJ; Jónsson 1999; Jónsson and Valdimarsson 2004; Våge et al. 2011). These are shown schematically in Fig. 1. The shelfbreak EGC is a well-known conduit of overflow water (e.g., Strass et al. 1993; Rudels et al. 2002),

but the other two currents have only recently been identified. Using a model, Våge et al. (2013) argued that a combination of bathymetry, baroclinic instability, and winds diverts a portion of the shelfbreak EGC into the interior forming the separated EGC, which resides at the base of the Iceland slope. Farther up the slope the NIJ also flows equatorward, following the 650-m isobath that is also the sill depth of Denmark Strait. As the separated EGC and NIJ approach the strait they merge, and, in the mean, appear as a single feature (Harden et al. 2016, Fig. 1). The final major current in Denmark Strait is the NIIC, which transports subtropical-origin water northward along the outer shelf of Iceland (Jónsson and Valdimarsson 2012).

Since DSOW is significantly denser than the ambient water of the northern Irminger Sea at sill depth, the overflow water descends, mixes, and entrains some of the lighter water south of the strait. During the descent there is conversion of potential energy into kinetic energy, which then cascades to smaller scales and influences the mixing. Independent of the descent, mesoscale processes may also impact the dynamics of the entrainment. The degree of entrainment is important as this helps to determine the properties of the final NADW product via modification of the dense source waters. The overflow plume south of Denmark Strait has been studied extensively, and it is known to be highly variable in space and time (e.g., Bruce 1995; Girton et al. 2001; Girton and Sanford 2003; von Appen et al. 2014b). This includes the generation of energetic cyclones in the mid- and upper

water column that are associated with lenses of overflow water descending the slope (Spall and Price 1998; von Appen et al. 2014b). The evolution of the gravity plume south of the strait and its parameter sensitivity has also been explored extensively (Jungclaus and Backhaus 1994; Krauss 1996; Krauss and Käse 1998; Jungclaus et al. 2001; Shi et al. 2001), but these studies all assumed time-independent flow in the strait and that all of the variability is generated downstream. Traditionally, the DSOW has been defined as water with potential density greater than 27.8 kg m^{-3} (Dickson and Brown 1994). Above this density horizon there are contributions to the NADW from dense water cascading over the east Greenland shelf downstream of Denmark Strait (Pickart et al. 2005; Falina et al. 2012; von Appen et al. 2014a) and from open-ocean convection in the Labrador Sea (e.g., Talley and McCartney 1982).

Over the years there have been numerous observational and theoretical studies investigating the processes that occur in the vicinity of the sill. The first attempt to measure the DSOW transport was reported by Worthington (1969), which revealed large variability in the velocities up to 1.5 m s^{-1} near the sill at a dominant period of 2–3 days. Since 1996, moorings have been maintained in the central part of the strait more or less continuously to monitor the transport and properties of the DSOW. Jochumsen et al. (2012) calculated that, in the mean, there are 3.4 Sv (1 Sv $\equiv 10^6$ m^3 s^{-1}) of overflow water denser than 27.8 kg m^{-3} leaving Denmark Strait. Notably, however, both the transport and hydrographic structure of the overflow south of Denmark Strait vary strongly on time scales of only a few days (Ross 1978; Bruce 1995; Käse et al. 2003). Dating back to Cooper (1955), the term "bolus" has been used to describe lenses of dense overflow water that intermittently pass through the strait. Bruce (1995) used the term "pulse" for an intermittent increase in near-bottom velocity. However, such features have only been loosely defined. Different generation mechanisms for the typical variability of a few days in the strait have been proposed, including baroclinic instability of the overflow (Smith 1976) and fluctuations of a surface jet passing through the strait (Fristedt et al. 1999). In the Faroe Bank Channel, the other main conduit of overflow water from the Nordic Seas to the North Atlantic, oscillations of the flow with periods of 2.5–5 days have been observed. These were attributed to topographic Rossby waves propagating through the strait (Darelius et al. 2011).

Using a collection of over 100 hydrographic sections occupied across the sill, Mastropole et al. (2017) recently devised an objective definition of a bolus in Denmark Strait based on its cross-sectional area and stratification. Using this definition, Mastropole et al. (2017) determined that the boluses are confined to the deepest part of the sill, typically banked on the western side of the trough. Such boluses were present in more than 40% of the hydrographic sections, implying that they are a very common feature of the DSOW crossing the sill. However, Mastropole et al. (2017) did not have any corresponding velocity data, so the kinematics and dynamics of the features have remained unexplored from an observational standpoint. Based on a numerical model, Jungclaus et al. (2001) concluded that the boluses are associated with anticyclonic flow.

In this study, we augment the collection of hydrographic sections used by Mastropole et al. (2017) with 6 yr of mooring data from the sill to more thoroughly investigate the type of mesoscale variability associated with the flow of DSOW. In addition to the well-known boluses that pass through the strait, here we identify and describe a previously unknown feature that we refer to as a pulse. As the name implies, this is characterized by an increase in velocity of the overflow, but, in contrast to the boluses, the overflow layer thins during the pulses. We compare the hydrographic and kinematic structure of the two classes of mesoscale variability and make some inferences concerning their dynamics. We begin by presenting the mooring and CTD data used in the study (section 2). Then we examine the conditions in Denmark Strait in the presence of overflow boluses (section 3) and overflow pulses (section 4). Finally, we discuss possible implications for the overflow transport and the downstream impacts of the mesoscale features that occur in Denmark Strait (section 5).

2. Data and methods

a. Mooring data in Denmark Strait

Mooring DS1 has been maintained at the 650-m isobath in the deepest part of the Denmark Strait sill (66°4.6'N, 27°5.6'W) since 1996 by the Marine Research Institute of Iceland. For the present study, we use data from summer 2005 to summer 2011, which represents 6 yr of data (there were no data for 2006–07). While this represents only a subset of the total record, 6 yr is more than sufficient to illuminate the features of interest in this mesoscale study. The mooring contains an upward-facing, 75-kHz Long Ranger RDI acoustic Doppler current profiler (ADCP) measuring near-bottom temperature (648-m depth) and velocity in 16-m bins between 80- and 630-m depth once per hour. Details about the mooring can be found in Jochumsen et al. (2012). The amplitude of the semidiurnal tide is a little less than half of the standard deviation of the velocity records in Denmark Strait. However, it only leads to typical tidal excursions of 2–3 km that do not significantly affect the transport through the strait (Macrander et al. 2007).

Therefore, the M_2 (12.42 h) and S_2 (12.00 h) tides were removed from the hourly velocity records using a tidal harmonic fit (T_TIDE; Pawlowicz et al. 2002). The mean flow at DS1 is southwestward. Based on this, plus the observed current ellipses, we defined the along-stream direction x as 210°T (southwestward, positive toward the Irminger Sea). The cross-stream direction y (right-hand coordinate system) is southeastward (toward Iceland).

Recently, side-lobe contaminations for newer versions of the 75-kHz Long Ranger ADCP have been reported for situations in which the instrument is moored close to a rocky (highly reflective) bottom (Nunes et al. 2016). The contamination results in an underestimation of the velocities in the bins that are within ≈ 200 m of the instrument. This applies for the ADCPs used in this study from 2007 to 2011, while the ADCP deployed during 2005–06 is an older model not subject to such contamination. We verified that the results presented below are not qualitatively impacted by the side-lobe interference by performing analogous calculations using the 2005–06 data alone. There are, however, some slight (quantitative) impacts that are noted at the appropriate points in the text.

b. Mooring data at the Spill Jet line

Mooring data from south of the sill are used in the study. From September 2007 to October 2008, an array of seven moorings was maintained across the east Greenland shelf/slope (Fig. 1). This location is known as the Spill Jet line since the East Greenland Spill Jet was first identified there (Pickart et al. 2005). We use the bottom temperature records from MicroCATs on the four deepest moorings. Details about the array and the time series can be found in von Appen et al. (2014b).

c. Hydrographic sections along the Látrabjarg line

The so-called Látrabjarg section extends across Denmark Strait near the location of the sill (Fig. 1) and has been occupied many times over the years. Von Appen et al. (2014a) and Mastropole et al. (2017) compiled all known occupations of the line between 1990 and 2012 (111 total). A table of the occupations is given in Mastropole et al. (2017). Some of the transects are shorter, extending from Iceland to the deepest part of the strait, while some reach entirely across the strait. The conductivity–temperature–depth (CTD) sections were quality controlled and then interpolated onto a regular grid of 2.5 km in the horizontal by 10 m in the vertical [see Mastropole et al. (2017) for details]. We make use of this gridded product in the present study.

d. Identification of the overflow water layer

To isolate the overflow water it is necessary to adequately define the interface between this layer and the water above.
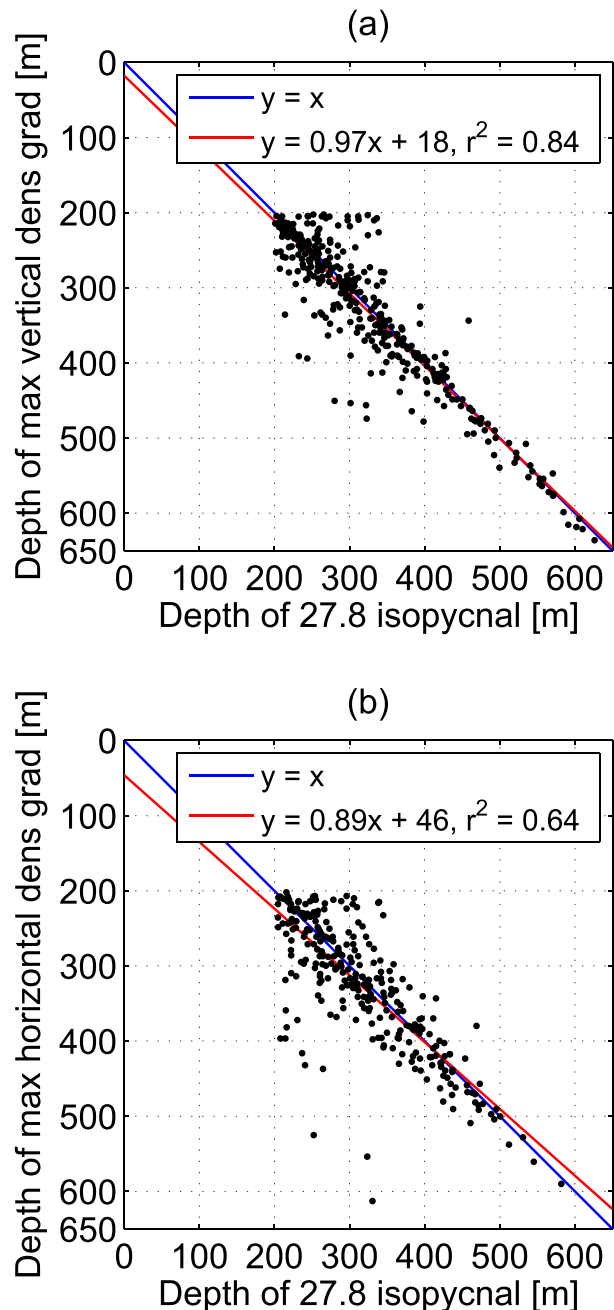

FIG. 2. Depth (m) of the 27.8 kg m^{-3} isopycnal vs (a) the depth of the maximum vertical density gradient and (b) the depth of the maximum horizontal density gradient. The individual realizations where both properties are deeper than 200 m are shown as are the one-to-one correlations (blue lines) and the least squares fits (red lines).

Macrander et al. (2007) considered three possible diagnostics of this interface based on the assumption that there is a relatively sharp density contrast at this depth and that there is a significant difference in advective speeds between the layers. The latter implies that there should be a
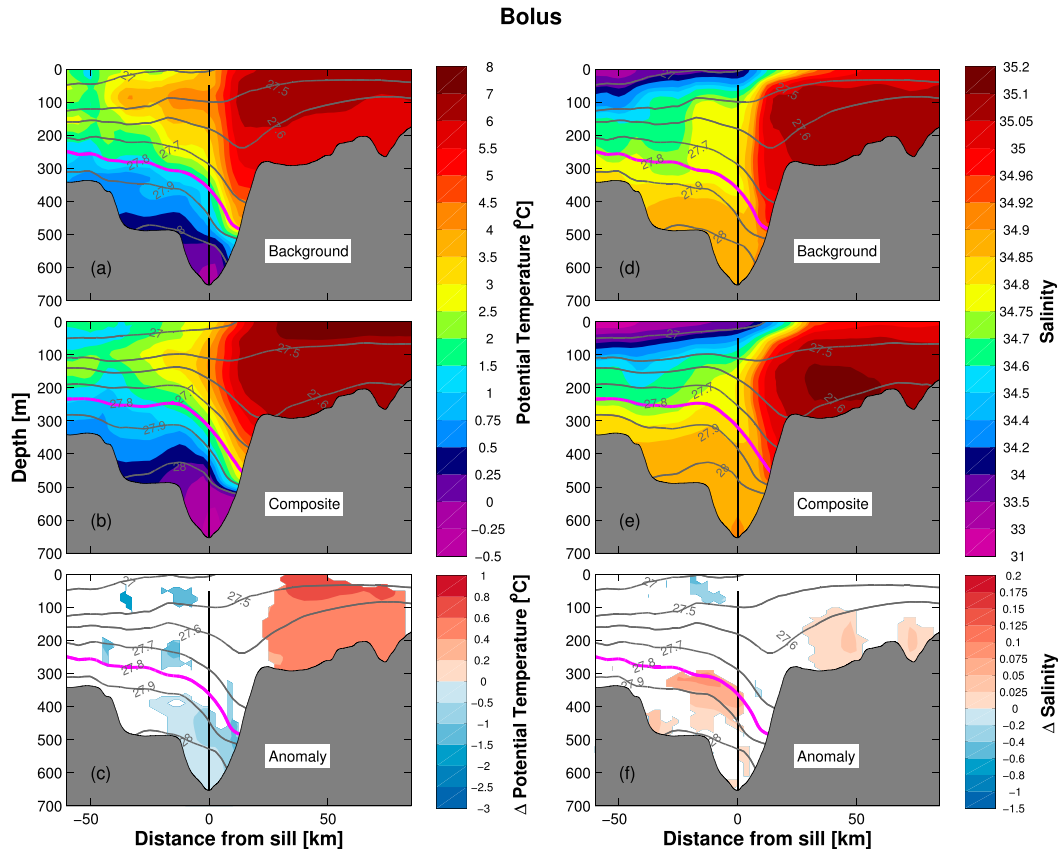
Bolus

FIG. 3. Hydrography along the Látrabjarg section [(left) west and (right) east] during boluses compared to the background state. (a),(b),(c) Potential temperature (°C) and (d),(e),(f) salinity, each overlain by potential density contours (kg m^{-3}). (a) and (d) show the background. (b) and (e) show the composite bolus. (c) and (f) show the anomaly of potential temperature/salinity for the bolus minus the background, overlain by the background potential density. The location of mooring DS1 is shown as a black line.

maximum in the vertical shear of the horizontal velocity that can be recorded by an ADCP. This was the first diagnostic considered by Macrander et al. (2007). The second diagnostic is that there should be a maximum in acoustic backscatter at this level due to a congregation of zooplankton (i.e., scatterers) on the gradient between the two water masses. Finally, a pressure inverted echo sounder was considered that could be calibrated to identify the interface height using hydrographic profiles from the area. Macrander et al. (2007) found that the three diagnostics agreed well with each other and could be used to successfully detect changes in the overflow layer height on time scales of a few hours and longer.

For this study, we use the maximum vertical shear in horizontal velocity as a measure of the overflow height. Since we have many more hydrographic sections than were available to Macrander et al. (2007), we were able to investigate more thoroughly the relationship between vertical shear and DSOW layer height. For each

Látrabjarg transect, the potential density profiles from the CTD stations (no gridding was performed) were used to determine 1) the depth of the 27.8 kg m^{-3} isopycnal, 2) the depth of the maximum vertical gradient of density, and 3) the depth of the maximum horizontal gradient of density at the deepest part of the Denmark Strait sill (i.e., where mooring DS1 was located). As seen in Fig. 2, both the depth of maximum stratification (point 2) and maximum horizontal density gradient (point 3) agree relatively well with the depth of the 27.8 kg m^{-3} isopycnal (the near-surface layer was excluded from this calculation). Both correlations are quite tight when the DSOW interface is near the bottom, although the relationship degrades somewhat as the interface height increases. By thermal wind, the maximum in horizontal density gradient is proportional to a maximum in the vertical shear of velocity; hence, Fig. 2b justifies our use of ADCP shear to determine the overflow layer height. (We note that while the magnitude of the maximum vertical shear may be

affected by the side-lobe contamination, its vertical location is not.)

3. Overflow boluses

We focus first on the most commonly observed mesoscale feature of the overflow water in Denmark Strait: boluses. As noted above, these features occur intermittently at the sill on time scales of a few days (e.g., Ross 1978; Bruce 1995; Käse et al. 2003). Recently, Mastropole et al. (2017) elucidated aspects of the boluses using the same collection of shipboard sections considered here. We now contrast the hydrographic conditions in the strait when boluses are present versus the background state, using the Látrabjarg sections. Following that, we employ the mooring data to investigate the circulation associated with these features.

a. Overflow boluses in the hydrographic sections

Mastropole et al. (2017) used three criteria to identify boluses in the hydrographic sections at the sill. The overflow water in question had to be weakly stratified ($N^2 < 2 \times 10^{-6}\,s^{-2}$), it needed to extend 150 m or more above sill depth, and the cross-sectional area of the feature had to occupy at least 65% of the trough ($y = -12$ to 13 km) that represents the deepest part of the sill. Based on this definition, 41% of the Látrabjarg sections contained boluses. The bolus frequency is not sensitive to the exact cutoff values used here, and the qualitative discussion below is independent of these choices. To determine the canonical hydrographic structure of the features, we computed a composite vertical section of the 46 transects containing boluses. This is compared to the background state in Denmark Strait (Fig. 3). The background is taken to be the composite of all transects that did not contain either a bolus or a pulse (the other dominant mesoscale feature that is investigated below in section 4).

The most conspicuous aspect of a bolus is the increased amount of cold water in the bottom of the trough. Using an end-member analysis, Mastropole et al. (2017) determined that these features contain predominantly Arctic-origin water, the coldest and densest overflow water. The boluses are also saltier than the ambient water in the trough (cf. Figs. 3d and 3e). The mean displacement of isopycnals associated with the passage of a bolus is quantified in Fig. 4. One sees that, in the center of the trough, the isopycnals are deflected upward by more than 50 m at depths greater than 400 m, and there is even significant upward displacement at depths above the overflow layer (as shallow as 200 m).

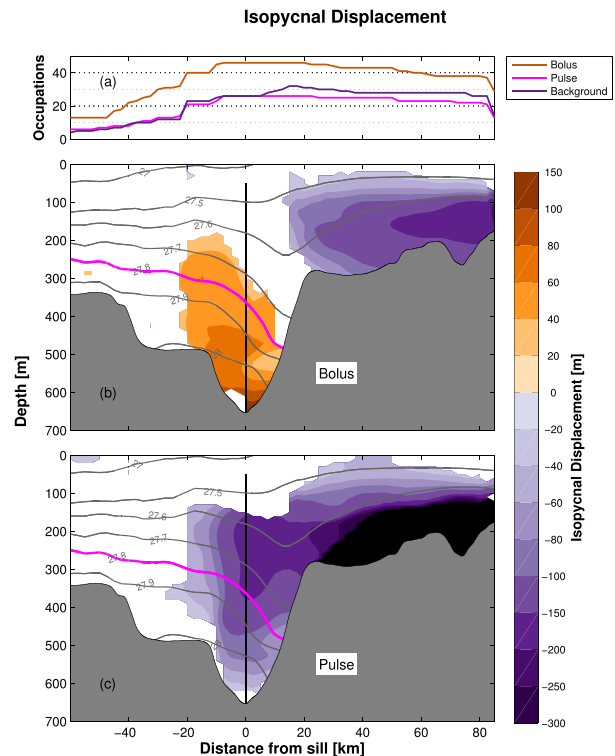We quantify the impact of the boluses by computing the anomaly between the background state and the

FIG. 4. (a) Number of occupations of the Látrabjarg line for the different cases. (b),(c) Isopycnal displacement due to the mesoscale features relative to the background. The depth (color), where a particular isopycnal is located in (b) the bolus case and (c) the pulse case, minus its depth in the background state, overlain by the isopycnals in the background case (contours).

bolus composite sections (Figs. 3c and 3f). Regions where the anomaly is not significant based on a Student's *t* test with 90% confidence are masked white. While the boluses are generally colder and saltier than the background, the biggest temperature difference occurs on the eastern flank of the trough because in the mean the coldest and densest DSOW is banked on the western side of the trough (so there is less change on that side). The biggest salinity difference, on the other hand, occurs in the overflow layer on the western flank of the trough. The other region of significant anomaly is on the Iceland shelf where the Irminger water appears to be warmer and saltier. However, this is due to the temporal distribution of the bolus sections. In particular, there are significantly more bolus occupations in the fall when the Irminger water is seasonally warmest and saltiest. When we remove some of the fall occupations so as to make the data coverage more uniform in time and thereby reduce seasonal biases, the anomaly on the Iceland shelf disappears. We stress, however, that the bolus anomaly signal in the trough does not change, which is consistent with the fact that there is no
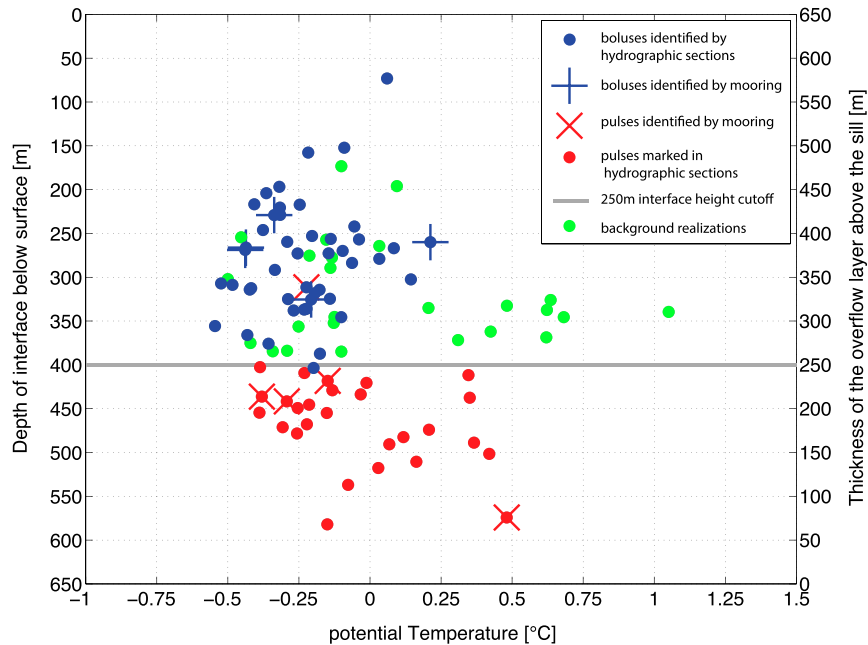
FIG. 5. Thickness of the overflow water layer ($>27.8\,\mathrm{kg\,m^{-3}}$) as a function of near-bottom potential temperature in the vicinity of DS1 from the hydrographic occupations (see text). Boluses contain weakly stratified fluid ($N^2 < 2 \times 10^{-6}\,\mathrm{s^{-2}}$) and were identified according to Mastropole et al. (2017). Pulses have interface thicknesses of less than 250 m. The background cases are the remaining points. Also shown are the boluses and pulses that were identified in the mooring (see the legend).

seasonality to the overflow water (Dickson and Brown 1994; Jónsson 1999; Jochumsen et al. 2012).

b. Overflow boluses in the mooring record

Unfortunately, it is not possible to detect the passage of boluses using the mooring data alone. This is partly because, as shown above, the technique of using the velocity shear to detect the height of the overflow layer is less accurate for large interface heights (which is the case for boluses). However, more importantly, the information provided by the mooring records is insufficient. For each of the Látrabjarg sections, we tabulated the value of temperature at the bottom of the trough (at the closest grid point to the mooring location) and compared this to the depth of the overflow interface at the same location (the height of the $27.8\,\mathrm{kg\,m^{-3}}$ isopycnal; Fig. 5). This represents what the mooring would measure if the shear metric from the ADCP data were perfect. The blue circles in the figure denote when boluses were present (46 total). As expected, these points correspond to cold temperatures and large interface heights (the upper-left quadrant of the plot). Notably, however, the combination of cold bottom temperatures and large interface heights does not by itself imply the presence of a bolus. This is due either to the stratification not being weak enough or the cross-sectional area not being large enough (or both).

As such, the green circles in the upper-left quadrant of the plot denote some of the realizations of the background state (the red symbols are discussed in the next section).

There were 10 occupations of the Látrabjarg line that captured a bolus during the time that the mooring was deployed. However, the mooring records showed inconsistent signals during five of these time periods, so we only consider the remaining five events that are marked in Fig. 5. (There are a number of possible reasons why some of the events did not show up clearly in the mooring time series, including weak currents, insufficient signal to noise ratios, and nonsmoothly evolving cross-stream velocities.) A compositing procedure was then applied to the remaining events to characterize the response of the water column to the passage of such a feature. Based on visual inspection of the mooring records, the time corresponding to a change in cross-stream velocity direction was determined for each event, which we assume to be associated with the center of the bolus. The time axis was then transformed to hours before/after the passage of the center. Then the events were averaged to form the composite, which extends from 36 h before the center of the bolus to 36 h after. We considered bottom temperature, along-stream velocity (see section 2a for the definition of along stream), cross-stream velocity, and interface height. The results are displayed in Fig. 6.
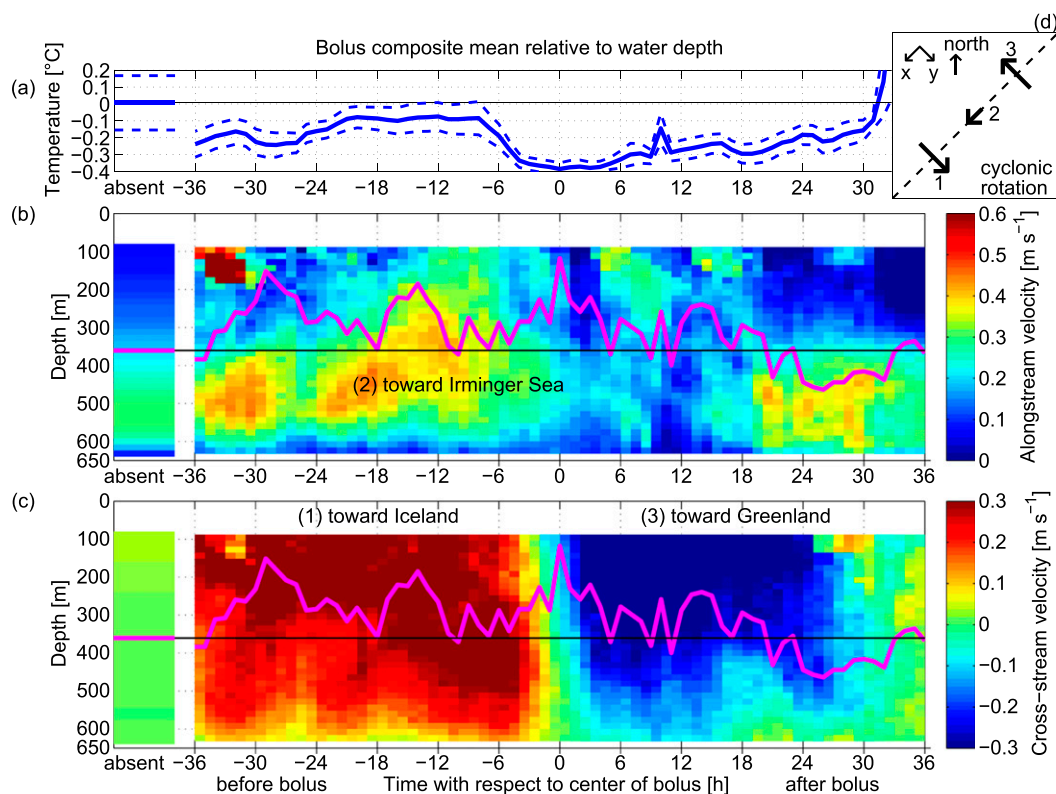
FIG. 6. Composite of the five boluses relative to water depth: (a) near-bottom temperature (°C; solid line indicates mean, dashed line indicates standard error). (b) Along-stream velocity (m s^{-1}) throughout the water column. The magenta line corresponds to the interface height. The *x* axis corresponds to the time with respect to the center of the bolus. The situation in the absence of the boluses is shown on the left. (c) As in (b), but for cross-stream velocity (m s^{-1}). (d) The cyclonic sense of the rotation is sketched: First, positive cross-stream velocity toward Iceland is registered. Then, weak positive along-stream velocity toward the Irminger Sea is registered. Finally, negative cross-stream velocity toward Greenland is registered. The orientation of the rotated coordinate system (*x*: along-stream, *y*: cross-stream) and the north direction is also shown in (d).

Not surprisingly, the passage of the bolus corresponds to a marked decrease in the bottom temperature at the sill, with a mean value of approximately −0.4°C at the center of the feature. In each of the panels of Fig. 6 we have indicated the background value of the given variable on the left of the plot (i.e., the average value of the quantity when the boluses are absent). The background bottom temperature is close to 0°C. The along-stream velocity and interface height are noisier than the temperature response, but a clear signal emerges. The along-stream velocity of the overflow layer increases from >0.3 to >0.4 m s^{-1} shortly before the passage of the bolus center, and, as expected, the interface height increases. (The along-stream velocities in the first ≈150 m above the bottom are likely larger than shown in Fig. 6 due to the side-lobe contamination discussed above.) The average vertical deflection of the interface is 50–60 m, which is in line with the composite hydrographic section shown earlier (Fig. 4a).

The clearest kinematic signal of the bolus is associated with the cross-stream velocity. As the center of the

feature approaches, the flow at the mooring site is directed toward Iceland, with a peak speed of 0.3 m s^{-1}. It then changes abruptly to flow toward Greenland after the center passes by, with a similar magnitude. This means that there is a cyclonic circulation associated with the bolus, which is shown schematically in the inset (Fig. 6d). We suspect, however, that this is not simply a cyclone passing over the mooring site. If that were the case then the expected direction of the along-stream velocity would depend on the distance from the eddy center: no azimuthal flow at zero cross-stream offset, negative (poleward) along-stream flow due to the azimuthal component on the Iceland side of the center, and positive (equatorward) along-stream flow on the Greenland side. Our ability to assess this is obviously limited by the fact that there is only one mooring, but since the mooring is in the center of a narrow trough (i.e., constrained topographically), it is likely close to the center of the feature—yet there is enhanced equatorward flow. Furthermore, the cross-stream
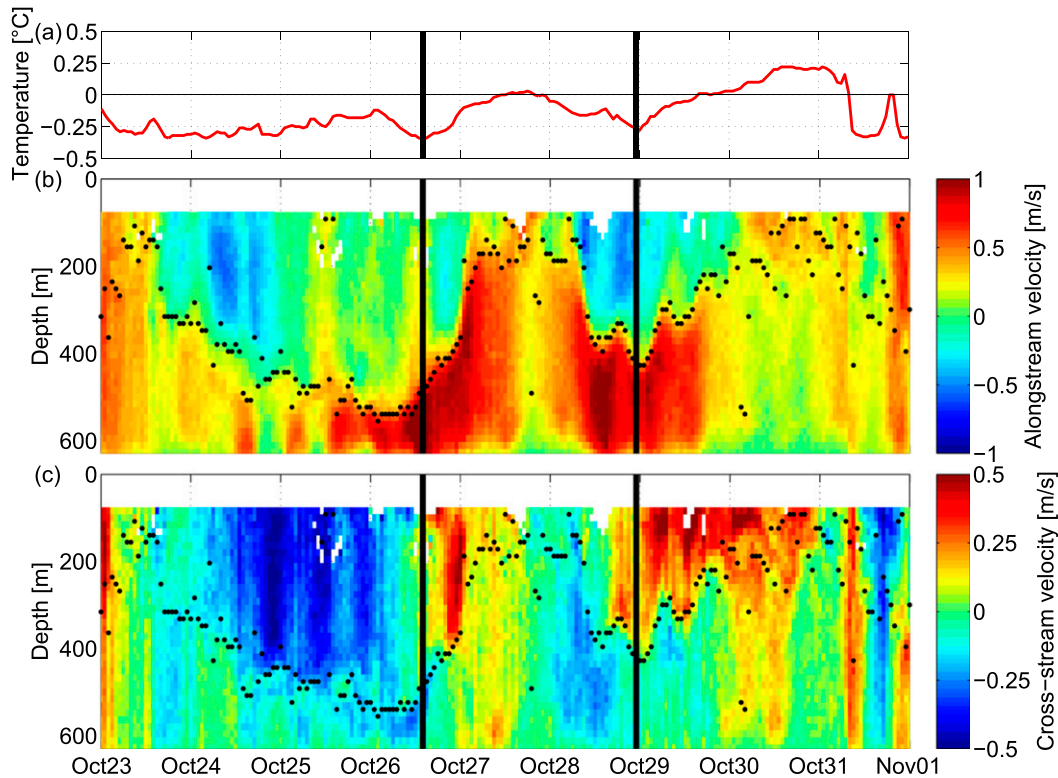
FIG. 7. Detection of overflow water pulses in Denmark Strait. The (a) near-bottom temperature (°C) as well as the (b) along-stream velocity (m s^{-1}; positive toward the Irminger Sea) and (c) cross-stream velocity (m s^{-1}; positive toward Iceland) records of the ADCP on DS1 are shown for a period of 9 days in 2007. The interface between the DSOW and the overlying intermediate waters is marked by black dots. The two identified pulses are marked with vertical black lines.

velocity is strongest in the upper layer, while the along-stream velocity signal is confined to the overflow layer.

This situation is similar to the cyclonic features observed downstream of the sill in the deep western boundary current (DWBC), known as DSOW cyclones. Using the mooring data from the Spill Jet line (Fig. 1), von Appen et al. (2014b) diagnosed these features. They showed that the equatorward propagation speed is greater than the swirl speed, meaning that the azimuthal flow in the upper layer is not strong enough to trap the fluid there. The interpretation is that as lenses of dense overflow water pass by, the local response in the upper layer is a cyclonic circulation. This is consistent with the theory of Swaters and Flierl (1991) and the laboratory experiments of Whitehead et al. (1990). Using a numerical model, Spall and Price (1998) demonstrated that DSOW cyclones spin up because of the stretching of the water column (in particular the intermediate layer) downstream of the sill. In their model the flow of dense water descending from the sill was steady in time, meaning that the features were not triggered by variations in the overflow. Our results demonstrate that mesoscale variability, with similar dynamics, does exist at the sill,

which likely is related to the presence of the DSOW cyclones downstream. This is discussed further in section 5.

4. Overflow pulses

We now demonstrate that there is a second type of mesoscale process that regularly occurs in Denmark Strait, which we refer to as a pulse. This terminology is used because the feature is associated with a strong, temporary increase in overflow speed (much larger than that associated with a bolus). Unlike the boluses, however, the pulses are easily detected in the velocity record from the mooring, whereas their property (temperature/salinity) signal in the hydrographic sections is not pronounced enough to be distinguishable. As such, we start with a presentation of the mooring data, followed by what can be deduced about these features from the Látrabjarg transects.

a. Overflow pulses in the mooring record

Visual inspection of the mooring records clearly reveals the occurrence of pulses of overflow water on short time scales. An example of this is shown in Fig. 7, which displays a 9-day span of the raw time series of the ADCP
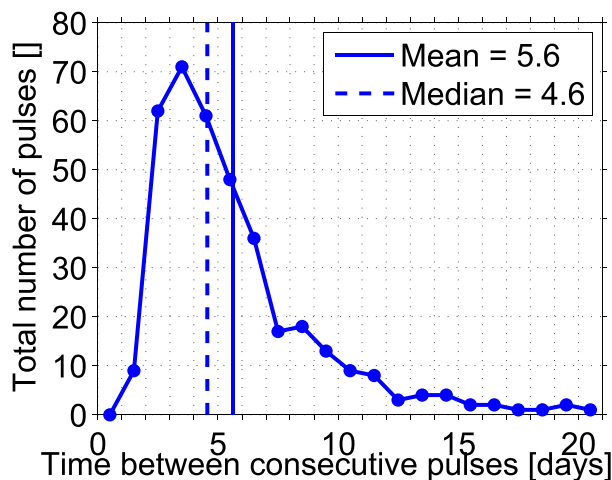
FIG. 8. Histogram of separation time in days between consecutive pulses.

data. The depth of the maximum vertical shear of the along-stream velocity is marked by black dots. The vertical shear is relatively well defined from time step to time step when the interface is relatively deep (i.e., closer to the bottom). Conversely, when the interface is relatively high in the water column, the identification becomes less clear and the deduced interface height between consecutive time steps is not smooth, consistent with the decreased correlation at these depths (Fig. 2). One sees that during this 9-day period there are two instances of enhanced along-stream flow of dense water (i.e., below the interface): one during 26 October and again during 29 October (marked by the black lines in the figure). Both instances corresponded to a minimum in interface height, a change in sign of the cross-stream flow from negative to positive, and a decrease in bottom temperature. We thus defined two velocity criteria: increased along-stream flow and a change in the cross-stream flow from negative to positive. These criteria, along with the requirement of a minimum in interface height, were used to identify these events in the time series (the bottom temperature signal was not required). It was attempted to devise an automated procedure to search for pulses, but this was not successful. Thus, we used the visual inspection mechanism noting that this may favor features similar to our preconception.

Inspection of the 6 yr of mooring data revealed the occurrence of 374 pulses. The time between consecutive pulses is a long-tailed distribution (Fig. 8). The pulses are at least 1 day apart, and there are periods of 15 or 20 days when no pulses are present. Since the distribution is skewed and long tailed, the mean is larger than both the median and the mode, and, on average, a pulse occurs at the mooring site every 5.6 days. There is also

no discernible seasonal signal in the frequency of the pulses, which implies that the generation mechanism of the pulses is a process without seasonal variation.

To get a canonical view of the pulses, we employed the following compositing procedure. At every time step in the record the interface height was determined from the maximum of the vertical shear of the along-stream velocity. Each of the pulses has a center time, which was visually determined from the time series. A 3D matrix was then set up with the first dimension corresponding to vertical distance from the interface, the second dimension corresponding to the temporal offset from the pulse center time, and the third dimension identifying the pulse number (1 to 374). The data were then averaged over all pulses to obtain the composite. The result is displayed (Fig. 9) relative to the composite evolution of the depth of the interface height (magenta line). As was done for the bolus composite (Fig. 6), we plot the value of the state in the absence of pulses on the left-hand side of the figure. (The effect of the side-lobe contamination is reduced in this composite because of the technique of averaging relative to the interface height.)

The first thing to note is that, like the boluses, pulses correspond to a decrease in near-bottom temperature (Fig. 9a), although the magnitude of the temperature difference for a pulse [$O(0.1)°C$] is significantly less than that for a bolus [$O(0.4)°C$]. Other aspects of the pulses are quite different than the boluses. In Figs. 9b and 9c, we plot the composite along-stream and cross-stream velocity, respectively, along with the mean interface depth. Note that the y axis is water column depth, even though the averaging of the velocities was done relative to the interface height. This preserves the large shear at the interface that gets blurred out if the compositing is done with respect to depth. (This compositing with respect to the interface height could not be done for the boluses because of the ill-defined progression of the interface.) As a typical pulse arrives, the interface height starts to decrease, reaching a minimum near the center of the feature before rising again toward the background value. The along-stream velocity of the overflow layer increases markedly, with maximum values exceeding $0.6 \, \text{m s}^{-1}$. At the leading edge of the pulse, in the upper part of the water column, there is strong flow toward Greenland (up to $0.3 \, \text{m s}^{-1}$), followed by equally strong flow toward Iceland at the trailing edge. Hence, while a bolus corresponds to a thickening of the overflow layer with cyclonic rotation, a pulse is associated with a thinning of the overflow layer and anticyclonic rotation (Fig. 9d).

As discussed above, the existence of boluses in Denmark Strait is well documented in the literature. To our knowledge, however, this is the first time that pulses have been identified, and, clearly, they are also a dominant
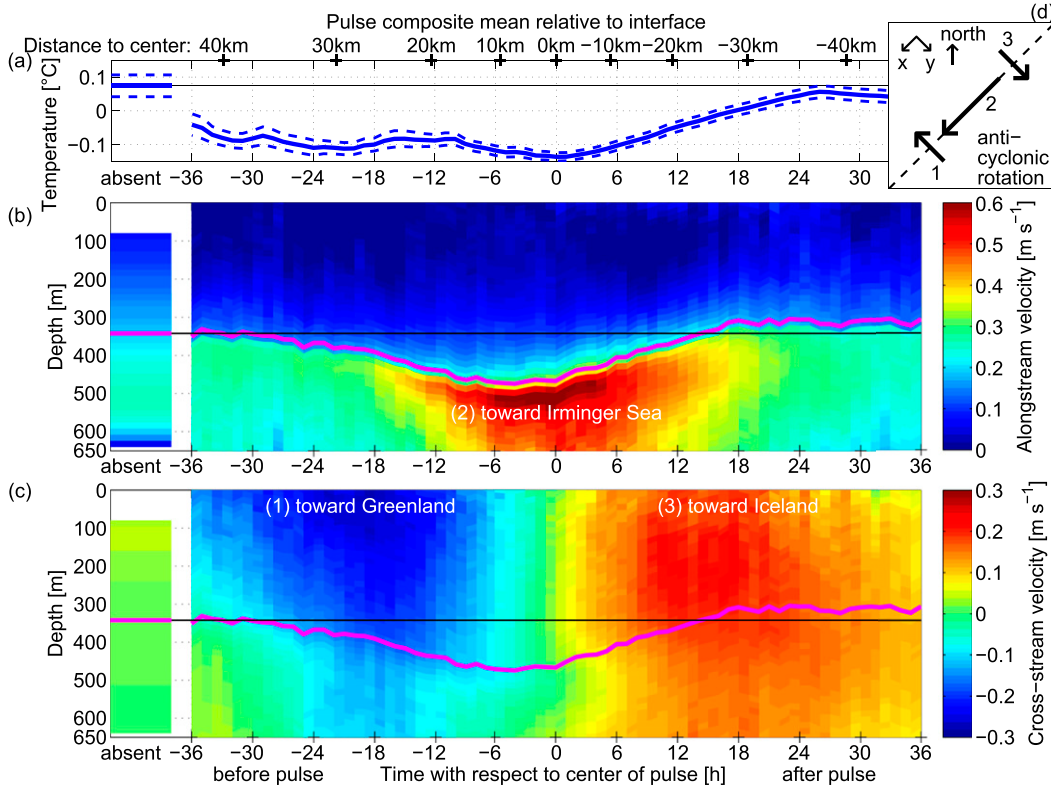
FIG. 9. As in Fig. 6, but for the composite of 374 pulses relative to interface height. Note the finer scale of the *y* axis in (a) compared to Fig. 6. (d) The anticyclonic sense of the rotation is sketched: First, negative cross-stream velocity toward Greenland is registered. Then, positive along-stream velocity toward the Irminger Sea is registered. Finally, positive cross-stream velocity toward Iceland is registered.

source of mesoscale variability at the sill. Typically, coherent eddies are considered to be features where the propagation of fluid (either trapped or not) occurs in the same depth as the rotational velocities. As is the case for the boluses, the pulses do not appear to be coherent eddies (anticyclones in this case) propagating through the strait. The along-stream flow is again confined to the overflow layer, while the cross-stream flow is largest in the layer above. Hence, dynamics similar to what is known to occur south of Denmark Strait (Swaters and Flierl 1991; von Appen et al. 2014b) may be at work involving the response of the upper water column to an anomaly in the flow of DSOW (whether it is a thickening or thinning of the layer).

b. Overflow pulses in the hydrographic sections

We now use the Látrabjarg transects to investigate the hydrographic structure of the pulses. Unlike boluses, however, which are quite evident in the individual vertical sections (particularly for temperature; see Mastropole et al. 2017), the anomalous thinning of the overflow layer is less well defined in a shipboard crossing. Therefore, we identified those transects that were occupied while the

mooring was in the water that corresponded to a time period that a pulse was present (based on the above analysis). Unfortunately this was the case for only five of the transects. These occupations are marked on Fig. 5 (red x's). In four of the five sections the interface height (27.8 kg m^{-3} isopycnal) was depressed.

Based on this, we assumed that all of the hydrographic occupations where the overflow layer was less than 250 m thick sampled a pulse, which is the only requirement for the identification of a pulse in the hydrographic record. We note that since the overflow layer is anomalously thin during the presence of pulses, it is also more stratified than in the bolus case. This is why the criterion of weak stratification is not applied for the pulses. The identified occupations are marked by the red circles in Fig. 5 (one of the bolus occupations has an interface height slightly less than 250 m). While the canonical progression of a pulse derived from the mooring records shows a small reduction of the bottom temperature to −0.1°C (Fig. 9a), the actual distribution associated with the 374 pulses is similar to a normal distribution with a mean of 0°C and standard deviation of 0.25°C. This agrees fairly well with the −0.5° to 0.5°C distribution of bottom temperatures
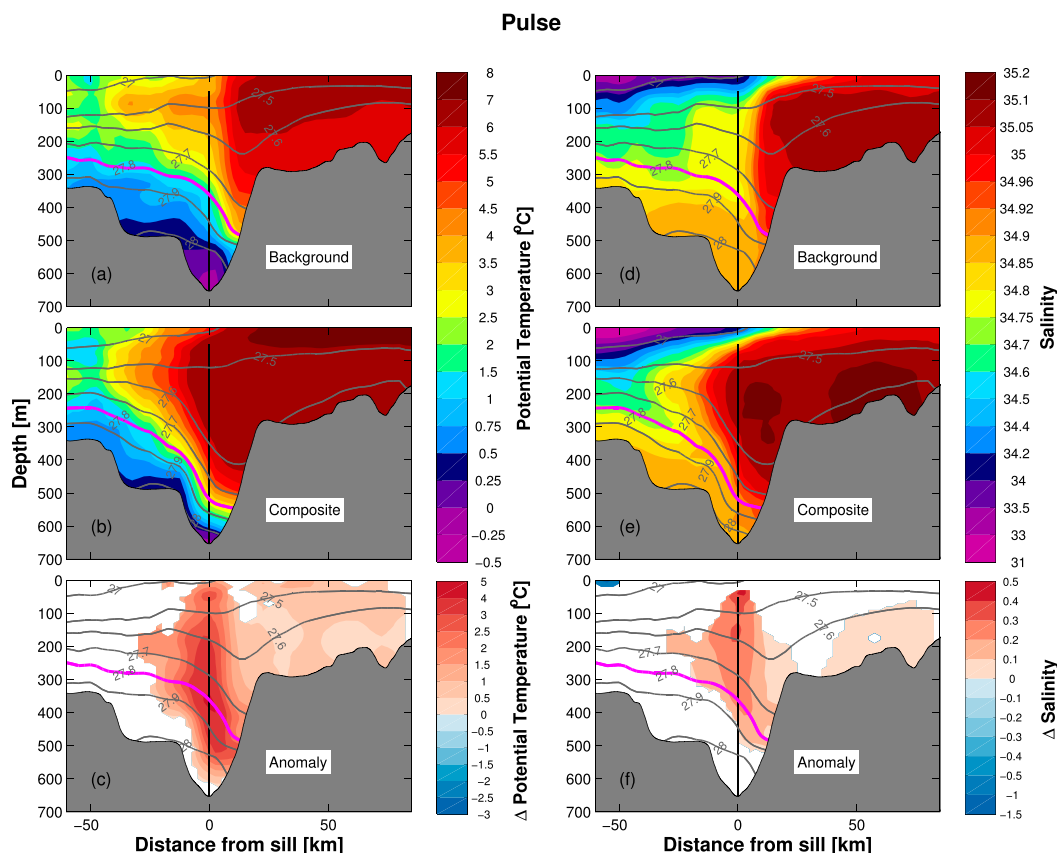
Pulse

FIG. 10. As in Fig. 3, but for the composite hydrography during pulses compared to the background state.

near the mooring site from the presumed pulse hydrographic occupations (red circles in Fig. 5). It also implies that individual pulses do not have a clear signal in bottom temperature (recall that the bottom temperature signal was not necessary to define a pulse in the mooring record). Note that the hydrographic transects representing the background conditions in Denmark Strait correspond to those occupations that did not sample a bolus or a pulse (green dots in Fig. 5).

To determine the typical hydrographic structure of a pulse, we composited the 28 hydrographic occupations corresponding to the red dots in Fig. 5. The result is displayed in Fig. 10. The thinning of the overflow layer is quite evident. The isopycnals are depressed as much as 90 m within the DSOW (Fig. 4), although the greatest deflection (>100 m) occurs in the middle of the water column above the overflow layer. This is different than the boluses, where the largest isopycnal displacement occurs within the overflow water (cf. Figs. 4b and 4c). Notably, even though the mooring records indicate a slight cooling near the bottom when a pulse occurs, the hydrographic composite reveals that most of the DSOW within the trough warms as the feature passes by. This is particularly evident in the anomaly section of Fig. 10c,

which shows an increase of up to 3°C (the near-bottom temperature anomaly in this plot is not significant, consistent with the fact that the mooring measured only a small decrease in bottom temperature). By contrast, there is little change in the salinity of the DSOW within a pulse (Fig. 10f).

The most striking feature in the pulse anomaly sections is a narrow region in the trough where a large part of the water column becomes warmer and saltier (extending well above the overflow layer). This is due to a westward shift in the hydrographic front between the subtropical Irminger water and the colder, fresher water to the west (cf. the composite background and pulse sections). Note also that the Irminger water on the Iceland shelf becomes warmer and saltier. Importantly, these signals are not the result of data coverage. Even when the fall occupations are removed from the pulse hydrographic composite—when the Irminger water is seasonally the warmest and saltiest—the anomaly plot shows the same result. Hence, this implies that a pulse of overflow water in Denmark Strait coincides with a westward displacement of the NIIC of approximately 20 km. We note that, in the upper part of the water column at DS1, there are cross-stream velocities of

$\approx 0.3\,\mathrm{m\,s}^{-1}$ for roughly 18 h both before and after the pulse (Fig. 9), equivalent to a distance of about 20 km, thus consistent with the frontal displacement seen in the hydrographic composite. The positive cross-stream flow after the passage of the pulse will advect the front back toward Iceland. Although we do not have velocity data on the Iceland shelf, the lateral displacement of the hydrographic front also suggests that the northward flow of the NIIC increases at the same time, bringing warmer and saltier water from south of the sill into Denmark Strait. The notion that there is a dynamical link between the mesoscale variability of the overflow water and fluctuations of the NIIC is intriguing and deserves further study. Specifically, it is of interest whether there is causality in that the NIIC front moves westward to occupy ''space'' made available by the thinning of the overflow or conversely in that the overflow is being compressed by the westward movement of the front. A forcing of the overflow water by a southward surface jet in Denmark Strait has previously been proposed by Fristedt et al. (1999), raising the possibility that our observations are a manifestation of that.

5. Summary and discussion

We have demonstrated that there are two distinct sources of mesoscale variability in Denmark Strait: boluses and pulses. While the existence of the former feature has been known for decades, we quantified its temperature signal and determined that it is associated with cyclonic rotation and a modest increase in along-stream speed of approximately $0.1\,\mathrm{m\,s}^{-1}$. When a bolus passes through the strait the interface height of the overflow layer increases by 50–60 m, and the bottom temperature decreases by $O(0.4)°C$. By contrast, pulses are characterized by a strong increase in along-stream speed of $>0.25\,\mathrm{m\,s}^{-1}$, a decrease in interface height of up to 90 m, and very little signal in bottom temperature. These features have not been previously identified and are associated with anticyclonic vorticity. Both the boluses and pulses have the strongest along-stream signal in the overflow layer, while the strongest cross-stream velocities occur above the DSOW. In this sense neither feature can be characterized as a simple eddy propagating through the strait, and their dynamics appear to be similar to that ascribed to the mesoscale variability observed downstream in the deep western boundary current.

Hydraulic control of the overflow transport has been considered in the past (e.g., Nikolopoulos et al. 2003), but it is not clear whether the transport is hydraulically controlled or controlled by other dynamics such as the mesoscale variability described here, topographic Rossby waves, or surface jet dynamics. Thus, future investigations will need to establish the causal relationships in Denmark Strait and whether the control is local to the strait or remote such as through hydraulics. With regard to the current system upstream of Denmark Strait (Fig. 1), boluses are composed mainly of Arctic-origin water (Mastropole et al. 2017), which is transported by the NIJ (and not the EGC). This would seem to suggest that these features originate from the NIJ, and mooring data from the northwest Iceland slope indicate energetic mesoscale variability in the jet (B. Harden 2016, personal communication). It is unclear at this point, however, which of the upstream currents (if any) are responsible for the pulses.

a. Implications for overflow transport

Although we had available to us only a single mooring in the center of Denmark Strait, the additional information from the shipboard transects enables us to make inferences about the transport of the two mesoscale situations relative to the background state. The average along-stream velocity of the overflow layer measured by the mooring during background conditions is $\approx 0.20\,\mathrm{m\,s}^{-1}$. When boluses are present, this increases slightly to $>0.22\,\mathrm{m\,s}^{-1}$, while for pulses the increase is much greater: $>0.47\,\mathrm{m\,s}^{-1}$ (in both instances the time period of the average is taken to be $\pm 12\,$h from the center of the feature). The cross-sectional area of the overflow layer in each case (background, bolus, pulse) is computed from the composite vertical sections (Figs. 3, 10), where the lateral limits are the 500-m isobath on either side of the trough ($y = -12$ to 13 km), and the upper boundary is the $27.8\,\mathrm{kg\,m}^{-3}$ isopycnal. The resulting cross-sectional areas are $6.3\,\mathrm{km}^2$ for the background, $7.6\,\mathrm{km}^2$ during boluses, and $3.5\,\mathrm{km}^2$ during pulses. Multiplying velocity times area yields a background transport of 1.3 Sv, a bolus transport of 1.7 Sv, and a pulse transport of 1.6 Sv. Hence, while the two mesoscale situations are qualitatively different—fast flow over a small area for the pulse and slower flow over a large area for the bolus—these effects compensate, resulting in similar transports that are 30%–40% larger than the background. The reader should note that although the values given here (for all three states) are likely biased a bit low due to the side-lobe contamination, the fractional differences are not affected.

A second (shorter term) mooring in the strait situated roughly 10 km toward Greenland from DS1 was considered by Jochumsen et al. (2012), and the total average transport of overflow water from the two moorings was calculated to be 3.4 Sv [which is in line with the value reported by Harden et al. (2016) using data from a mooring array upstream of the sill]. The relation of the transport determined from the two moorings at the sill was also compared to the contribution from DS1 alone,
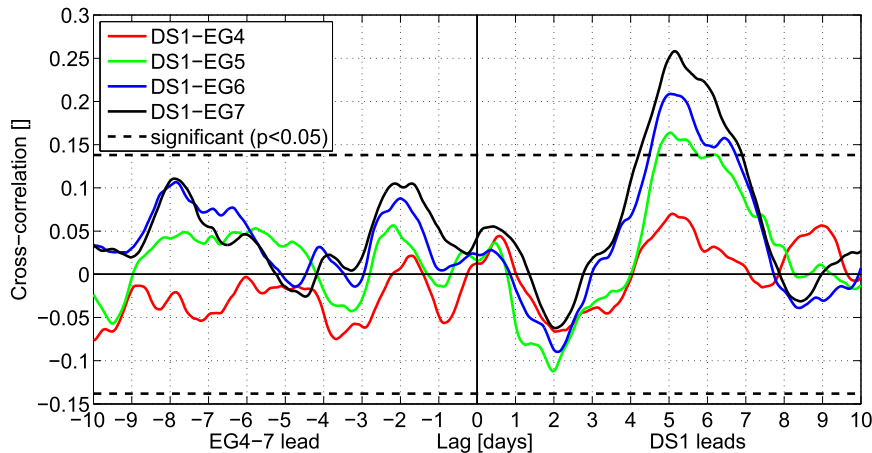
FIG. 11. Cross-correlation of bottom temperature records at moorings DS1 and at EG4–7 (see Fig. 1 for the locations of the moorings).

and the DS1 value is in line with our estimates here [note, however, that Jochumsen et al. (2012) did not isolate periods of mesoscale variability]. Overflow water is also present on the east Greenland shelf, which is likely flowing toward the North Atlantic. However, at present it is unknown if there is any relationship between the flow on the shelf and that in the trough; hence, we cannot determine the full transport of either the boluses or pulses.

b. Downstream impacts

Downstream of the sill, the dominant mesoscale variability of the overflow water is due to the passage of DSOW cyclones (Spall and Price 1998; von Appen et al. 2014b). Using time series data from the year-long mooring array located at the Spill Jet line (Fig. 1), von Appen et al. (2014b) determined that these features pass by the site on average every 2.1 days. Is there a relationship between the downstream cyclones and the mesoscale features at the sill presented here? While we know how often pulses occur in the strait from the DS1 mooring records, the boluses are not detectable in the time series. However, the Látrabjarg transects allow us to deduce their frequency of occurrence. Of the 111 sections, 46 are bolus occupations and 28 are presumed to be pulse realizations. This means that boluses are slightly more prevalent than pulses, that is, $46/28 = 1.6$ times as many boluses as pulses were identified. Since pulses pass through the strait every 5.6 days, this suggests that boluses go by on average every 3.4 days. This in turn implies that a mesoscale feature (pulse or bolus) passes through Denmark Strait every 2.1 days, which is precisely the frequency of DSOW cyclones passing by the Spill Jet array.

If this relationship is causal, it implies that both types of mesoscale disturbances in Denmark Strait lead to the generation of cyclones downstream. Comparison of the

bottom temperature records at the two mooring sites reveals a significant correlation (Fig. 11; where significance here is assessed from a Monte Carlo simulation of the time series with 4000 iterations). The bottom temperatures at the three deepest downstream locations on the east Greenland slope (sites EG5–EG7 at 1150- to 1600-m depth) are significantly correlated with DS1 at a lag of about 5 days. Dividing this lag by the distance of 280 km results in a speed of $0.65\,\mathrm{m\,s^{-1}}$, which is in good agreement to the propagation speed of the overflow water cyclones at the Spill Jet line of $0.72\,\mathrm{m\,s^{-1}}$ deduced by von Appen et al. (2014b). The correlation at 5-day lag is positive, indicating that cold fluctuations in Denmark Strait are followed by cold signals downstream and likewise for warm fluctuations. This agrees with Jochumsen et al. (2015), who find similar lags from 20-day low-pass filtered records using independent downstream data. [We note that the difference in the absolute values of the correlations between Fig. 11 and Jochumsen et al. (2015) is due to the large amount of incoherent variance that is removed by Jochumsen et al.'s (2015) low-pass filtering.] We also investigated the frequency band over which the signals are coherent using the Thompson multitaper method and found that the 5-day lag is due to mesoscale motions rather than variability with longer periods.

Based on this evidence, we propose the following scenario: Boluses are associated with cyclonic vorticity in Denmark Strait and contain very dense water. As such, when they descend into the Irminger Basin they stretch to form strong cyclones that reside in deep water (here we assume that the entrainment is linear with respect to density difference so that denser features sink deeper). On the other hand, pulses are anticyclonic and contain relatively lighter overflow water at the sill. During descent this would result in weaker cyclones

(assuming that the cyclonic vorticity due to the stretching overcomes the anticyclonic initial condition). At the same time the smaller density anomaly means that they would end up at shallower depths. At the Spill Jet line the observed cyclones are distributed over a wide range of bottom depths, from 500 to 1600 m (von Appen et al. 2014b). Hence, our hypothesis offers an explanation for this distribution as well as the frequency of occurrence of the DSOW cyclones downstream in the deep western boundary current. We note that such a scenario is different than the model results of Spall and Price (1998), whereby a steady overflow leads to the generation of cyclones. Further work is required to determine if there is indeed a one-to-one correspondence between the features at the sill and the downstream cyclones and if the boluses and pulses are somehow dynamically linked to one another and/or the north Icelandic Irminger Current.

REFERENCES

Bruce, J., 1995: Eddies southwest of the Denmark Strait. *Deep-Sea Res. I*, **42**, 13–17, doi:10.1016/0967-0637(94)00040-Y.

Cooper, L., 1955: Deep water movements in the North Atlantic as a link between climatic changes around Iceland and biological productivity of the English Channel and Celtic Sea. *J. Mar. Res.*, **14**, 347–362.

Darelius, E., I. Fer, and D. Quadfasel, 2011: Faroe Bank Channel overflow: Mesoscale variability. *J. Phys. Oceanogr.*, **41**, 2137–2154, doi:10.1175/JPO-D-11-035.1.

Dickson, R., and J. Brown, 1994: The production of North Atlantic Deep Water: Sources, rates, and pathways. *J. Geophys. Res.*, **99**, 12 319–12 341, doi:10.1029/94JC00530.

Falina, A., A. Sarafanov, H. Mercier, P. Lherminier, A. Sokov, and N. Daniault, 2012: On the cascading of dense shelf waters in the Irminger Sea. *J. Phys. Oceanogr.*, **42**, 2254–2267, doi:10.1175/JPO-D-12-012.1.

Fristedt, T., R. Hietala, and P. Lundberg, 1999: Stability properties of a barotropic surface-water jet observed in the Denmark Strait. *Tellus*, **51A**, 979–989, doi:10.1034/j.1600-0870.1999.00030.x.

Girton, J., and T. Sanford, 2003: Descent and modification of the overflow plume in the Denmark Strait. *J. Phys. Oceanogr.*, **33**, 1351–1364, doi:10.1175/1520-0485(2003)033<1351:DAMOTO>2.0.CO;2.

——, ——, and R. Käse, 2001: Synoptic sections of the Denmark Strait overflow. *Geophys. Res. Lett.*, **28**, 1619–1622, doi:10.1029/2000GL011970.

Hansen, B., and S. Østerhus, 2007: Faroe Bank Channel overflow 1995–2005. *Prog. Oceanogr.*, **75**, 817–856, doi:10.1016/j.pocean.2007.09.004.

Harden, B., and Coauthors, 2016: Upstream sources of the Denmark Strait overflow: Observations from a high-resolution mooring array. *Deep-Sea Res. I*, **112**, 94–112, doi:10.1016/j.dsr.2016.02.007.

Hattermann, T., P. E. Isachsen, W.-J. von Appen, J. Albretsen, and A. Sundfjord, 2016: Eddy-driven recirculation of Atlantic Water in Fram Strait. *Geophys. Res. Lett.*, **43**, 3406–3414, doi:10.1002/2016GL068323.

Jochumsen, K., D. Quadfasel, H. Valdimarsson, and S. Jónsson, 2012: Variability of the Denmark Strait overflow: Moored time series from 1996–2011. *J. Geophys. Res.*, **117**, C12003, doi:10.1029/2012JC008244.

——, M. Köllner, D. Quadfasel, S. Dye, B. Rudels, and H. Valdimarsson, 2015: On the origin and propagation of Denmark Strait overflow water anomalies in the Irminger Basin. *J. Geophys. Res. Oceans*, **120**, 1841–1855, doi:10.1002/2014JC010397.

Jónsson, S., 1999: The circulation in the northern part of the Denmark Strait and its variability. Int. Council for the Exploration of the Sea Tech. Rep. ICES CM 1999/L:06, 10 pp. [Available online at http://www.ices.dk/sites/pub/CM%20Doccuments/1999/L/L0699.pdf.]

——, and H. Valdimarsson, 2004: A new path for the Denmark Strait overflow water from the Iceland Sea to Denmark Strait. *Geophys. Res. Lett.*, **31**, L03305, doi:10.1029/2003GL019214.

——, and ——, 2012: Water mass transport variability to the North Icelandic shelf, 1994–2010. *ICES J. Mar. Sci.*, **69**, 809–815, doi:10.1093/icesjms/fss024.

Jungclaus, J., and J. Backhaus, 1994: Application of a transient reduced gravity plume model to the Denmark Strait overflow. *J. Geophys. Res.*, **99**, 12 375–12 396, doi:10.1029/94JC00528.

——, J. Hauser, and R. Käse, 2001: Cyclogenesis in the Denmark Strait overflow plume. *J. Phys. Oceanogr.*, **31**, 3214–3229, doi:10.1175/1520-0485(2001)031<3214:CITDSO>2.0.CO;2.

Käse, R., J. Girton, and T. Sanford, 2003: Structure and variability of the Denmark Strait overflow: Model and observations. *J. Geophys. Res.*, **108**, 3181, doi:10.1029/2002JC001548.

Krauss, W., 1996: A note on overflow eddies. *Deep-Sea Res. I*, **43**, 1661–1667, doi:10.1016/S0967-0637(96)00073-8.

——, and R. H. Käse, 1998: Eddy formation in the Denmark Strait overflow. *J. Geophys. Res.*, **103**, 15 525–15 538, doi:10.1029/98JC00785.

Macrander, A., R. Käse, U. Send, H. Valdimarsson, and S. Jónsson, 2007: Spatial and temporal structure of the Denmark Strait overflow revealed by acoustic observations. *Ocean Dyn.*, **57**, 75–89, doi:10.1007/s10236-007-0101-x.

Mastropole, D., R. S. Pickart, H. Valdimarsson, K. Våge, K. Jochumsen, and J. Girton, 2017: On the hydrography of Denmark Strait. *J. Geophys. Res. Oceans*, **122**, doi:10.1002/2016JC012007, in press.

Mauritzen, C., 1996: Production of dense overflow waters feeding the North Atlantic across the Greenland-Scotland Ridge. Part 1: Evidence for a revised circulation scheme. *Deep-Sea Res. I*, **43**, 769–806, doi:10.1016/0967-0637(96)00037-4.

Nikolopoulos, A., K. Borenäs, R. Hietala, and P. Lundberg, 2003: Hydraulic estimates of Denmark Strait overflow. *J. Geophys. Res.*, **108**, 3095, doi:10.1029/2001JC001283.

Nunes, N., M. Moritz, K. Jochumsen, D. Quadfasel, K. Larsen, H. Valdimarsson, and S. Jónsson, 2016: A revised estimate of

the Denmark Strait overflow. *Geophysical Research Abstracts*, Vol. 18, Abstract 13822. [Available online at http://meetingorganizer. copernicus.org/EGU2016/EGU2016-13822.pdf.]

Pawlowicz, R., B. Beardsley, and S. Lentz, 2002: Classical tidal harmonic analysis including error estimates in MATLAB using T_TIDE. *Comput. Geosci.*, **28**, 929–937, doi:10.1016/S0098-3004(02)00013-4.

Pickart, R., D. Torres, and P. Fratantoni, 2005: The East Greenland Spill Jet. *J. Phys. Oceanogr.*, **35**, 1037–1053, doi:10.1175/JPO2734.1.

Ross, C., 1978: Overflow variability in Denmark Strait. Int. Council for the Exploration of the Sea Tech. Rep. ICES CM 1978/C:21, 9 pp. [Available online at http://www.ices.dk/sites/pub/CM%20Doccuments/1978/C/1978_C21.pdf.]

Rudels, B., E. Fahrbach, J. Meincke, G. Budéus, and P. Eriksson, 2002: The East Greenland Current and its contribution to the Denmark Strait overflow. *ICES J. Mar. Sci.*, **59**, 1133–1154, doi:10.1006/jmsc.2002.1284.

Shi, X. B., L. P. Røed, and B. Hackett, 2001: Variability of the Denmark Strait overflow: A numerical study. *J. Geophys. Res.*, **106**, 22 277–22 294, doi:10.1029/2000JC000642.

Smith, P., 1976: Baroclinic instability in the Denmark Strait overflow. *J. Phys. Oceanogr.*, **6**, 355–371, doi:10.1175/1520-0485(1976)006<0355:BIITDS>2.0.CO;2.

Spall, M., and J. Price, 1998: Mesoscale variability in Denmark Strait: The PV outflow hypothesis. *J. Phys. Oceanogr.*, **28**, 1598–1623, doi:10.1175/1520-0485(1998)028<1598:MVIDST>2.0.CO;2.

Strass, V. H., E. Fahrbach, U. Schauer, and L. Sellmann, 1993: Formation of Denmark Strait overflow water by mixing in the East Greenland Current. *J. Geophys. Res.*, **98**, 6907–6919, doi:10.1029/92JC02732.

Swaters, G., and G. Flierl, 1991: Dynamics of ventilated coherent cold eddies on a sloping bottom. *J. Fluid Mech.*, **223**, 565–587, doi:10.1017/S0022112091001556.

Swift, J. H., and K. Aagaard, 1981: Seasonal transitions and water mass formation in the Iceland and Greenland Seas. *Deep-Sea Res.*, **28A**, 1107–1129, doi:10.1016/0198-0149(81)90050-9.

Talley, L., and M. McCartney, 1982: Distribution and circulation of Labrador Sea Water. *J. Phys. Oceanogr.*, **12**, 1189–1205, doi:10.1175/1520-0485(1982)012<1189:DACOLS>2.0.CO;2.

Våge, K., R. Pickart, M. Spall, H. Valdimarsson, S. Jónsson, D. Torres, S. Østerhus, and T. Eldevik, 2011: Significant role of the north Icelandic jet in the formation of Denmark Strait overflow water. *Nat. Geosci.*, **4**, 723–727, doi:10.1038/ngeo1234.

——, ——, ——, G. Moore, H. Valdimarsson, D. Torres, S. Erofeeva, and J. Nilsen, 2013: Revised circulation scheme north of the Denmark Strait. *Deep-Sea Res.*, **79**, 20–39, doi:10.1016/j.dsr.2013.05.007.

von Appen, W.-J., and Coauthors, 2014a: The East Greenland Spill Jet as an important component of the Atlantic meridional overturning circulation. *Deep-Sea Res. I*, **92**, 75–84, doi:10.1016/j.dsr.2014.06.002.

——, R. Pickart, K. Brink, and T. W. N. Haine, 2014b: Water column structure and statistics of Denmark Strait overflow water cyclones. *Deep-Sea Res. I*, **84**, 110–126, doi:10.1016/j.dsr.2013.10.007.

Whitehead, J., M. Stern, G. Flierl, and B. Klinger, 1990: Experimental observations of baroclinic eddies on a sloping bottom. *J. Geophys. Res.*, **95**, 9585–9610, doi:10.1029/JC095iC06p09585.

Worthington, L., 1969: An attempt to measure the volume transport of Norwegian Sea overflow water through the Denmark Strait. *Deep Sea Res.*, **16** (Suppl.), 421–432.